Chapter 7

The Standard Model Higgs Boson

Authors: Sara Bolognesi, Chiara Mariotti and Daniele Trocino

Revisors: Barbara Mele, Paolo Nason

7.1 Higgs Boson Mass

The Higgs boson mass is the only yet unknown free parameter of the SM. The Higgs in fact has never been observed experimentally and its mass cannot be predicted by the SM. It depends on the parameters v and λ, but while the former can be estimated by its relation with the constant G_F of Fermi's theory, the latter is characteristic of the field ϕ and cannot be determined other than measuring the Higgs mass itself. Both theoretical and experimental constraints exist, including those from direct search at colliders, in particular LEP.

7.1.1 Theoretical constraints

Theoretical constraints to the Higgs mass value [1)] can be found by imposing the energy scale Λ up to which the SM is valid, before the perturbation theory breaks down and non-SM phenomena emerge. The upper limit is obtained requiring that the running quartic coupling of Higgs potential λ remains finite up to the scale Λ (*triviality*). A lower limit is found instead by requiring that λ remains positive after the inclusion of radiative corrections, at least up to Λ: this implies that the Higgs potential is bounded from below, i.e. the minimum of such potential is an absolute minimum (*vacuum stability*). A looser

constraint is found by requiring such minimum to be local, instead of absolute (*metastability*). These theoretical bounds on the Higgs mass as a function of Λ are shown in Fig. 7.1.

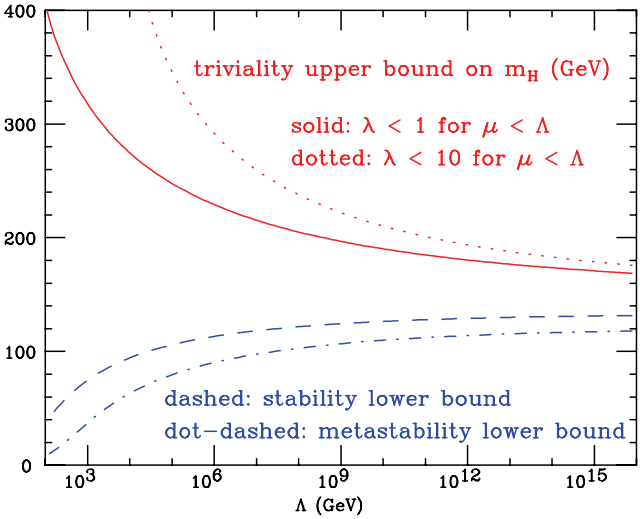

Figure 7.1: *Red line*: *triviality* bound (for different upper limits to λ); *blue line*: *vacuum stability* (or *metastability*) bound on the Higgs boson mass as a function of the new physics (or cut-off) scale Λ [1].

If the validity of the SM is assumed up to the Plank scale ($\Lambda \sim 10^{19}\ GeV$), the allowed Higgs mass range is between 130 and 190 GeV/c^2, while for $\Lambda \sim 1\ TeV$ the Higgs mass can be up to 700 GeV/c^2. On the basis of these results, the LHC has been designed for searches of the Higgs boson up to masses of $\sim 1\ TeV$. If the Higgs particle is not found in this mass range, then a more sophisticated explanation for the EWSB mechanism will be needed.

7.1.2 Experimental constraints

Bounds on the Higgs mass are also provided by measurement at LEP, SLC and Tevatron [2] (updated at July 2007). A lower bound at 114.4 GeV/c^2 (at 95% C.L.) has been established by direct searches at LEP [3]. Moreover, since the Higgs boson contributes to radiative corrections, many electroweak observables are logarithmically sensitive to M_H and can thus be used to constraint its mass. All the precision electroweak measurements performed by the four LEP experiments, SLD, CDF and D$\emptyset$ have been combined together and fitted, assuming

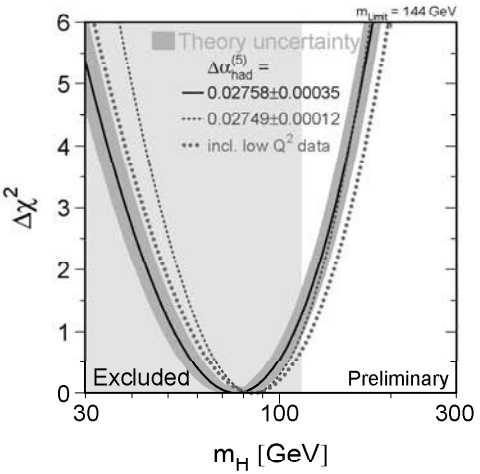

Figure 7.2: $\Delta\chi^2$ of the fit to the electroweak precision measurements of LEP, SLC and Tevatron as a function of the Higgs mass (July 2007). The solid line represents the result of the fit and the blue shaded band is the theoretical error from unknown higher-order corrections. The yellow area represents the region excluded by direct search.

the SM as the correct theory and using the Higgs mass as free parameter. The result of this procedure is summarized in Fig. 7.2, where $\Delta\chi^2 = \chi^2 - \chi^2_{min}$ is plotted as a function of M_H. The solid curve is the result of the fit, while the shaded band represents the theoretical uncertainty due to unknown higher order corrections.

As of Summer 2007, the indirectly measured value of the Higgs boson mass, corresponding to the minimum of the curve, is $M_H = 76^{+33}_{-24}\ GeV$ (at 68% C.L. for the black line in Fig. 7.2, thus not taking the theoretical uncertainty into account). An upper limit of 144 GeV can also be set (one-sided 95% C.L.) including the theoretical uncertainty; this limit increases to 182 GeV/c^2 when including the direct search limit of 114.4 GeV/c^2.

Such results are obviously model-dependent, as the loop corrections take into account only contributions from known physics. This result is thus well-grounded only within the SM theory and has always to be confirmed by the direct observation of the Higgs boson.

7.2 Standard Model Higgs Boson search at LHC

The experiments at the LHC will search for the Higgs boson within a mass range going from 100 GeV/c^2 to about 1 TeV. In this section, the main Higgs boson production and decay processes are described, in order to determine the most promising channels for the Higgs discovery at LHC.

While the Higgs boson mass is not predicted by the theory, the Higgs boson couplings to the fermions and bosons are predicted to be proportional to the corresponding particle masses (for fermions) or squared masses (for bosons). For this reason, the Higgs boson production and decay processes are dominated by channels involving the coupling of Higgs boson to heavy particles, mainly to $W^{\pm}$ and Z bosons and to the third generation of fermions. For what concerns the remaining gauge bosons, the Higgs boson does not couple to photons and gluons at tree level, but only by one-loop graphs where the main contribution is given by t loops for the $gg{\rightarrow}H$ channel and by W^+W^- and t loops for the $\gamma\gamma{\rightarrow}H$ channel.

7.3 Higgs boson production

The main processes contributing to the Higgs boson production at a hadron collider are represented by the Feynman diagrams in Fig. 7.3. The corresponding cross sections for a center of mass energy $\sqrt{s} = 14\ TeV$, corresponding to the design value at the LHC, are shown in Fig. 7.4.

7.3.1 Gluon-gluon fusion

The gg fusion is the dominating mechanism for the Higgs boson production at the LHC over the whole Higgs boson mass spectrum. The process is shown in Fig. 7.3(a), with a t quark-loop as the main contribution.

The cross section for the basic gluon to Higgs boson process is [6)]

$$\sigma(gg \rightarrow H) = \frac{G_\mu \alpha_S^2(\mu_R^2)}{288\sqrt{2}\pi} \left| \frac{3}{4} \sum_q A_{1/2}^H(\tau_Q) \right|^2 , \tag{7.1}$$

where $A_{1/2}^H(\tau_Q)$ with $\tau_Q = M_H^2/4m_q^2$ is a form factor [7)].

The lowest order cross section has large corrections from higher order QCD diagrams. The increase in cross section from higher order diagrams is conventionally defined as the K-factor

$$K = \frac{\sigma_{NLO}}{\sigma_{LO}} \tag{7.2}$$

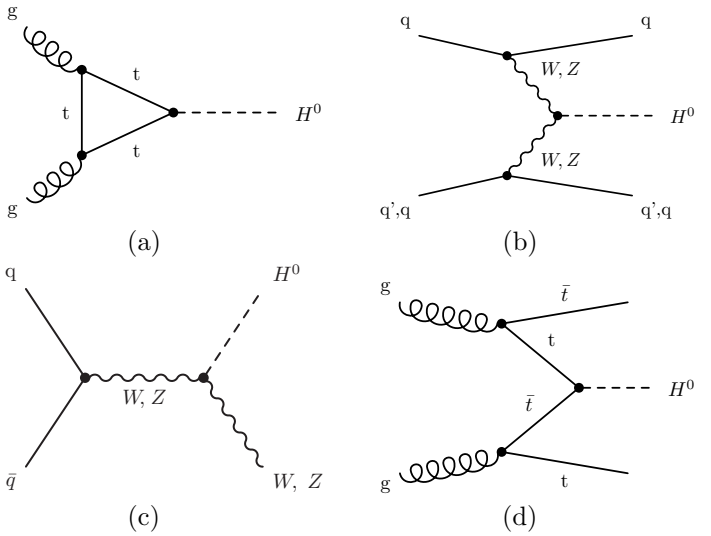

Figure 7.3: Higgs boson production mechanisms at tree level in proton-proton collisions: (a) gluon-gluon fusion; (b) VV fusion; (c) W and Z associated production (or *Higgsstrahlung*); (d) $t\bar{t}$ associated production.

where LO (NLO) refer to leading (next-to-leading) order results. The K-factor for gluon fusion is evaluated in Ref. [8] with a next-to-leading order calculation and it results $\sim$2.

The value of the cross section including the K-factor has two main uncertainties. The first is from the gluon structure function which still has large uncertainty in the low x region. The cross section using a large set of todays best available structure functions was calculated in Ref. [9] and the results differ by around 20% which can be taken as the theoretical uncertainty from the gluon structure function. At the time of data taking for LHC it can be expected to have much better structure functions available with data from HERA and the Tevatron.

Next-to-next-to leading order calculations are also available and show a further increase of about 10% to 30%. Other sources of uncertainty are the higher order corrections ($10 \div 20\%$ estimated).

The production of the Higgs boson through gluon fusion is sensitive to a fourth generation of quarks. Because the Higgs boson couples proportionally to the fermion mass, including a fourth generation of very heavy quarks will more than double the cross section.

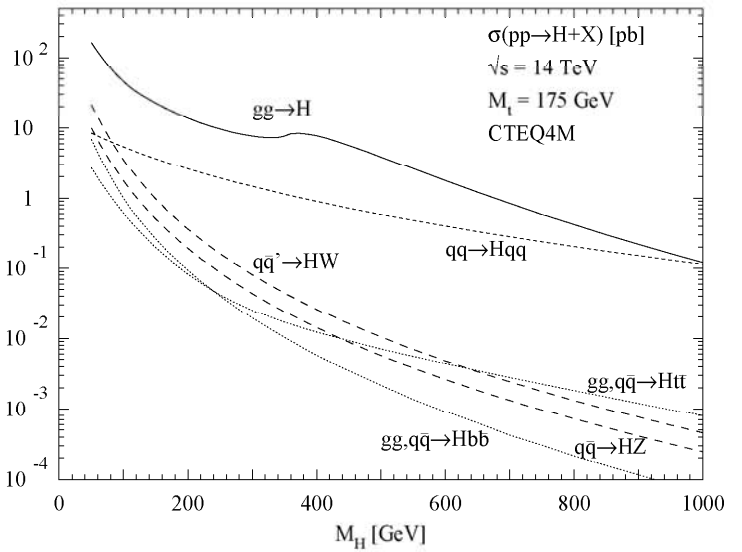

Figure 7.4: Higgs boson production cross sections at $\sqrt{s} = 14\ TeV$ as a function of the Higgs boson mass. The cross sections are calculated using HIGLU and other programs [4]; they contain higher order corrections and the CTEQ6m [5] p.d.f. has been adopted.

7.3.2 Vector boson fusion

The VV fusion (Fig. 7.3(b)) is the second contribution to the Higgs boson production cross section. It is about one order of magnitude lower than gg fusion for a large range of M_H values and the two processes become comparable only for very high Higgs boson masses ($\mathcal{O}(1\ TeV)$). However, this channel is very interesting because of its clear experimental signature: the presence of two spectator jets with high invariant mass in the forward region provides a powerful tool to tag the signal events and discriminate the backgrounds, thus improving the signal to background ratio, despite the low cross section. Moreover, both leading order and next-to-leading order cross sections for this process are known with small uncertainties and the higher order QCD corrections are quite small.

7.3.3 Associated production

In the *Higgsstrahlung* process (Fig. 7.3(c)), the Higgs boson is produced in association with a $W^{\pm}$ or Z boson, which can be used to tag the event. The

cross section for this process is several orders of magnitude lower than gg and VV fusion ones. The QCD corrections are quite large and the next-to-leading order cross section results to be increased by a factor of $1.2 \div 1.4$ with respect to the leading order one.

The last process, illustrated in Fig. 7.3(d), is the associated production of a Higgs boson with a $t\bar{t}$ pair. Also the cross section for this process is orders of magnitude lower than those of gg and VV fusion, but the presence of the $t\bar{t}$ pair in the final state can provide a good experimental signature. The higher order corrections increase the cross section of a factor of about 1.2.

7.4 Higgs boson decay

The branching ratios of the different Higgs boson decay channels are shown in Fig. 7.5 as a function of the Higgs boson mass. Fermionic decay modes dominate the branching ratio in the low mass region (up to $\sim$150 GeV/c^2). In particular, the channel $H \to b\bar{b}$ has the highest branching ratio since the b quark is the heaviest fermion available. When the decay channels into vector boson pairs open up, they quickly dominate. A peak in the $H \to W^+W^-$ decay is visible around 160 GeV/c^2, when the production of two on-shell W's becomes possible and the production of a real ZZ pair is still not allowed. At high masses ($\sim$350 GeV/c^2), also $t\bar{t}$ pairs can be produced.

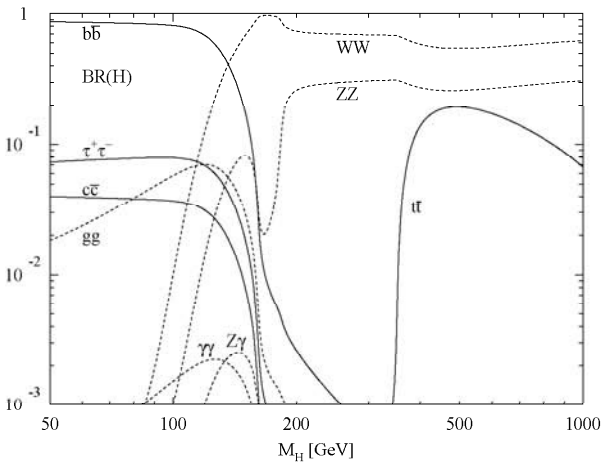

Figure 7.5: Branching ratios for different Higgs boson decay channels as a function of the Higgs boson mass. They are calculated with the program `HDECAY` [10] which includes the dominant higher order corrections to the decay width.

As shown in Fig. 7.5, the branching ratios change dramatically across the possible range of the Higgs boson mass requiring different strategies for the different Higgs boson mass range. The most promising decay channels for the Higgs boson discovery do not only depend on the corresponding branching ratios, but also on the capability of experimentally detecting the signal rejecting the backgrounds. Fully hadronic events are the most copious final states from Higgs boson decays. These decays can not be easily resolved when merged in QCD background, therefore topologies with leptons or photons are preferred, even if they have smaller branching ratio.

Such channels are illustrated in the following, depending on the Higgs boson mass range.

7.4.1 Low mass region

Though the branching ratio in this region is dominated by the Higgs boson decay into $b\bar{b}$, the background constituted by the di-jet production (more tan six order of magnitude higher than the signal) makes quite difficult to use this channel for a Higgs boson discovery. Some results from this channel can be obtained when the Higgs boson is produced in association with a $t\bar{t}$ or via *Higgsstrahlung*, since in this case the event has a clearer signature, despite its low cross section.

The most promising way of identifying a Higgs boson in the low mass region is to select the decay channel $H \to \gamma\gamma$. In spite of its lower branching ratio (around 10^{-3}), the two high energy photons constitute a very clear signature, which only suffers from the $q\bar{q} \to \gamma\gamma$ and $Z \to e^+e^-$ backgrounds or jets faking photons. The expected signal to background ratio is 10^{-2}, which make this channel much more attractive than the $b\bar{b}$ channel.

7.4.2 Intermediate mass region

For a Higgs boson mass value between $130 GeV/c^2 \leq M_H \leq 2M_Z$, the Higgs boson decays into $WW^{(*)}$ and ZZ^* open up and their branching ratios quickly increase. Thus the best channels in this mass region are $H \to WW^{(*)} \to 2\ell 2\nu$ and $H \to ZZ^* \to 4\ell$ with only one vector boson on-shell.

The branching ratio of $H \to WW^{(*)}$ is higher, because of the higher coupling of the Higgs boson to charged current with respect to neutral current. Moreover, this decay mode becomes particularly important in the mass region between $2M_W$ and $2M_Z$, where the Higgs boson can decay into two real W's (and not yet into two real Z's): its branching ratio is $\sim$1. Anyway, in such channel because of the presence of the two ν's in the final state, the Higgs boson mass cannot be reconstructed. Such measurement can be performed instead

when one W decays leptonically and the other one decays in two quarks. But, in this case, the final state suffers from the high hadronic background.

The decay $H \to ZZ^* \to 4\ell$, despite its lower branching ratio, offers a very clear experimental signature and high signal to background ratio. Furthermore, it allows to reconstruct the Higgs boson mass with high precision. Therefore, this channel seems to be the best candidate for a Higgs boson discovery in this mass range.

7.4.3 High mass region

This region corresponds to Higgs boson mass values above the $2M_Z$ threshold, where the Higgs boson can decay into a real ZZ pair. Though the $H \to ZZ$ width is still lower than $H \to WW$ one, a decay into four charged leptons (muons or electrons) is surely the "golden channel" for a high mass Higgs boson discovery.

The upper mass limit for detecting the Higgs boson in this decay channel is given by the reduced production rate and the increased width of the Higgs boson. As an example, less than 200 Higgs particles with $M_H = 700 GeV/c^2$ will decay in the $H \to ZZ \to 4\ell$ channel in a year at high luminosity and the large width will increase the difficulty to observe the mass peak.

In order to increase the sensitivity to a heavy Higgs boson production, decay channels with one boson decaying into jets or neutrinos can be also considered. The decay channel $H \to WW \to \ell\nu_\ell$jj, where j denotes a jet from a quark in the W decay, has a branching ratio just below 30%, yelding a rate some 50 times higher than the four lepton channel from $H \to ZZ$ decays. The decay channel $H \to ZZ \to \ell\bar{\ell}\nu_{\ell'}\bar{\nu}_{\ell'}$ which has a six times larger branching ratio than the four lepton channel could also be interesting.

7.4.4 Higgs boson total decay width

The total width of the Higgs boson resonance is shown in Fig. 7.6 as a function of M_H. Below the $2M_W$ threshold, the Higgs boson width is of the order of the MeV, then it rapidly increases, but remains lower than 1 GeV/c^2 up to $M_H \simeq 200\ GeV$: the low mass range is therefore the most challenging region, because the Higgs boson width is dominated by the experimental resolution.

In the high mass region ($M_H > 2M_Z$), the total Higgs boson width is dominated by the W^+W^- and ZZ partial widths, which can be written as

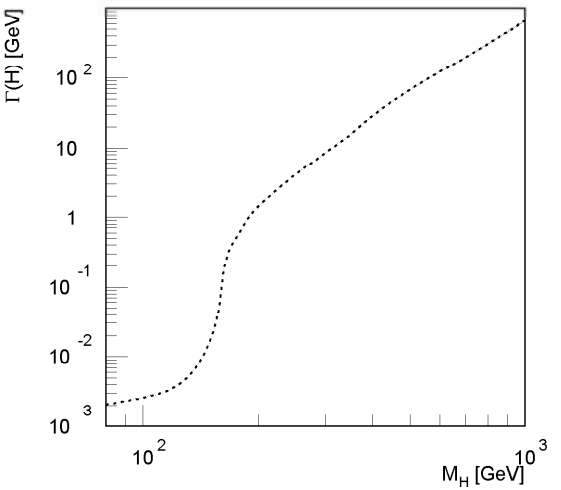

Figure 7.6: Higgs boson total decay width as a function of the Higgs boson mass.

follows:

$$\Gamma(H \to W^+W^-) = \frac{g^2}{64\pi}\frac{M_H^3}{M_W^2}\sqrt{1-x_W}\left(1 - x_W + \frac{3}{4}x_W^2\right) \quad (7.3)$$

$$\Gamma(H \to ZZ) = \frac{g^2}{128\pi}\frac{M_H^3}{M_W^2}\sqrt{1-x_Z}\left(1 - x_Z + \frac{3}{4}x_Z^2\right) \quad (7.4)$$

where

$$x_W = \frac{4M_W^2}{M_H^2}, \qquad x_W = \frac{4M_Z^2}{M_H^2}.$$

As the Higgs boson mass grows, $x_W,\ x_Z \to 0$ and the leading term in Eqs. 7.3 and 7.4 grows proportional to M_H^3. Summing over the W^+W^- and ZZ channels, the Higgs boson width in the high mass region can be written as

$$\Gamma(H \to VV) = \frac{3}{32\pi}\frac{M_H^3}{v^2}. \quad (7.5)$$

From Eq. 7.5, it results that $\Gamma_H \simeq M_H$ for $M_H \simeq 1\ TeV$. When M_H becomes larger than a TeV, therefore, it becomes experimentally very problematic to separate the Higgs boson resonance from the VV continuum. Actually, being the resonance width larger than its own mass, the Higgs boson cannot be

properly considered as a particle any more. In addition, if the Higgs boson mass is above 1 TeV, the SM predictions violate unitarity. All these considerations suggest the TeV as a limit to the Higgs boson mass: at the TeV scale at least, the Higgs boson must be observed, or new physics must emerge.

7.5 The Higgs search from the first fb^{-1} to 100 fb^{-1}

In this session the discovery strategies for the Standard Model Higgs boson are presented with the focus on the results with 1, 10 and 30 fb^{-1}, which should correspond respectively to about one year of data taking at the start-up luminosity and the first year and three years at low luminosity ($2 \times 10^{33} cm^{-2} s^{-1}$). Finally the significances for a Higgs discovery after 100 fb^{-1} are summarized.

7.6 $H \to \gamma\gamma$

If $M_H = 100 - 140$ GeV/c^2 the decay with the highest probability to observe it in $\gamma\gamma$. Even if the BR is very low, NLO BR ($\simeq 0.002$), we expect a narrow peak in 2 photon invariant mass (see Fig. 7.7). The amount of background is very high: Drell-Yan e^+e^-, $pp \to \gamma\gamma$ (irreducible), $pp \to jets + \gamma$ and $pp \to jets$ where one or more jets are misidentified as γ (reducible). In particular this last kind of background has a big dependence on the detector performance and it involves not well known QCD physics. Therefore there is a great deal of uncertainty in the benchmark estimate of significance and of needed luminosity (shown in Figures 7.10 and 7.11. However this will not be a systematic error on real data since the background will be precisely measured from the data themselves, exploiting the big $M(\gamma\gamma)$ sidebands signal free ($\simeq 1\%$).

For this channel the resolution on the electromagnetic calorimeters is critical, as it is the amount of material in front of them. In ATLAS and CMS there is about 1.5 X_0 of material in front of the electromagnetic calorimeter, that makes 50% of the electrons and photons loose more than 50% of their energy.

At LHC the longitudinal spread of the interaction vertexes is of 53 mm resulting in almost 2 Gev/c^2 smearing on M_H. The charged tracks in the event will allow the determination of the primary vertex with a 5 mm precision in most of the signal events.

7.7 $H \to b\bar{b}$

Experiments are putting a lot of effort in the search for a Higgs boson decaying into b quarks, in order to have an alternative channel with respect to the photonic one for low Higgs masses. The background is the production of $b\bar{b}$

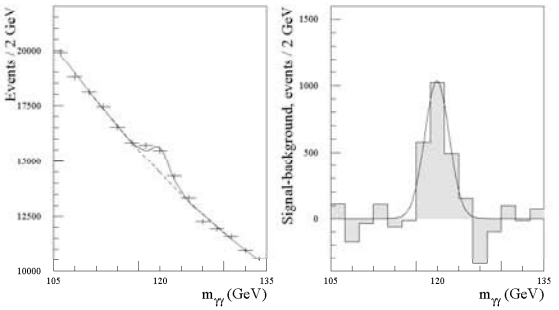

Figure 7.7: The $\gamma\gamma$ mass spectrum from ATLAS simulation with an integrated luminosity of 100 fb^{-1}. On the right after the background subtraction.

and $t\bar{t}$ pairs than it is impossible to think to be able to isolate a Higgs produced via gluon fusion. The Higgs boson production via $t\bar{t}$ fusion presents a possible solution. Three possible final state are taken into consideration: the fully leptonic: $H \to \bar{b}b, t \to \ell\nu b,\ t \to \ell\nu\bar{b}$, the semi-leptonic: $H \to \bar{b}b, t \to \bar{q}qb, t \to \ell\nu\bar{b}$ and the fully hadronic: $H \to \bar{b}b, t \to \bar{q}qb, \bar{t} \to \bar{q}q\bar{b}$ This signal will be recognized due to the presence of a high p_T lepton from one of the two W and missing energy and 4 b-tagged jets (of which two from the Higgs). The background will be high to due the presence of many jets in the event. The major backgrounds are the production of $ttbb$, Zbb, $tt + Njets$ and multi-jets QCD events. The main sources of uncertainty are the MC predictions, the jet energy scale the b-tagging efficiency.

A novel study for the search for a Higgs into $b\bar{b}$ [12] considers the production via Vector Boson Fusion in association with a photon. The final state is then characterized by two forward/backward jets, two b-jets and a central high p_T photon. The additional request of a photon in the detector increases drastically the signal over background ratio. Studies after detector effects are under way.

7.8 $H \to ZZ(^*) \to 4l$

These channels are very promising for the Higgs detection in the mass range 130 GeV-500 GeV, with the exception of a small interval near 160 GeV where the $H \to ZZ(^*)$ branching ratio (BR) has a big drop due to the opening of the WW on-shell production.

The main backgrounds are: $t\bar{t}$ ($\sigma \simeq 840\ pb$), $Zb\bar{b}$ ($\sigma \simeq 280\ pb$) usually

it is generated with CompHEP (gg and $q\bar{q}$ initial state), and the irreducible $ZZ(^*)/\gamma^*$ ($\sigma \simeq 30\ pb$) generated as well with CompHEP (both t ans s channel) to be compared with the $H \to ZZ(^*)$ cross section of about 10-50 pb. Zcc has been found to be negligible.

The trigger and the offline cuts applied in the analysis rely on the presence of isolated charged leptons coming from the primary vertex and with high transverse momentum. The Z mass peak is also a powerful feature: more than 50% (80%) of the events have at least one on-shell Z for $M(H) > 115$ (150) GeV. Requiring lepton isolation and cutting differently on the sorted p_T of the leptons the reducible background become negligible. The irreducible background can be partly cut away with cuts on angular variables (that are Higgs Mass dependence).

The studied final states are $2e2\mu$, 4μ and $4e$. The first has the biggest BR while the second is the cleanest one. The main concern of the last channel is the presence, for low Higgs masses, of very soft electrons, well below the range for which the reconstruction will be best controlled via single Z and W measurements. The main systematics error sources are: the choice of the PDF and the QCD scale, the NLO versus the LO dynamics, the isolation cut and its efficiency, the electron reconstruction efficiency, the energy and momentum scale and the charge identification. It is important to normalize with the data itself by using two other control samples: the Drell-Yan and the side bands of the Higgs spectra that suffer from low statistics.

In Figures 7.10 and 7.11 the luminosity needed for a 5σ discovery and the significance achievable with 30 fb^{-1}, combining the three possible final states, is plotted as a function of the Higgs mass.

7.9 $H \to WW(^*) \to l\nu l\nu$

The leptonic decays of both the W in the ee, $e\mu$ and $\mu\mu$ combinations have been studied. The signal has a cross section of 0.5-2.3 pb with a peak at $M(H) = 160\ GeV$ but does not present an invariant mass peak due to presence of the two neutrinos. This channel present a very clean signature: 2 isolated high p_T leptons pointing to the primary vertex and high missing energy and no hadron activity. The main backgrounds are single and double top production ($\sigma \simeq 90\ pb$) and double boson production ($\sigma \simeq 15\ pb$), considering only the fully leptonic decays. The Drell-Yan background after the full selection should be less than 2% of the total background (there is no high missing energy). Figures 7.10 and 7.11 shows the luminosity needed for a 5σ discovery and the significance obtained with 30 fb^{-1} as a function of the Higgs mass.

The final state selection relies mainly on the request of high missing energy ($> 50\ GeV$) and on a central jet veto. The main kinematic peculiarity of this

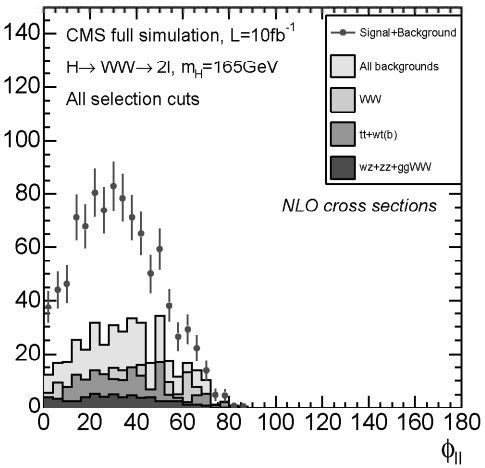

Figure 7.8: Distribution of the angle between the charged leptons in the transverse plane after all selection cuts (excluding the one on ϕ_{ll}), in $H \to WW(^*) \to l\nu l\nu$ signal (with $M(H) = 165\ GeV$) and in various backgrounds, with 10 fb^{-1} of integrated luminosity.

channel is the closeness of the two charged leptons due to the fact the Higgs boson is a scalar and that the V-A structure of the weak interaction. For this channel the correct simulation of the spin correlation matters (see Figure 7.8) The absence of the Higgs peak requires an high signal over background ratio and a good control of the background shape. Therefore a procedure to normalize the background from the data is necessary: a different signal free region for each background has been defined varying the analysis cuts. The uncertainties for the various backgrounds are between 15% and 20%, with the exception of single top and $gg \to WW$ processes for which it's not possible to find a good normalization region so that the systematics ($\simeq 30\%$) are dominated by MC theorethical errors.

7.10 Vector Boson Fusion Production

During the last years a lot of effort has been put on the Vector Boson Fusion production channels. These channels present a very clear signature given by the two forward and backward jets. The presence of these two jets together with the decay products of the Higgs allows a good rejection of dominant background coming from V+n jets, VV+n jets and $t\bar{t}$ production. The forward

and backward jets tend to be well separated in pseudo-rapidity and to have a very high invariant mass.

More generally the Vector Boson Fusion cross section (with or without a production of a Higgs particle) is an extremely interesting process to study because the cross section $\sigma(pp \to VVjj)$ and the polarizations of the VV pair depend sensitively on the presence or absence of a light Higgs in the physical spectrum. If a massive Higgs boson exists, a resonance will be observed in the VV invariant mass spectrum in correspondence of the Higgs mass. In absence of the Higgs particle, the Standard Model (SM) predicts that the scattering amplitude of longitudinally polarized vector boson grows linearly with s and violates unitarity at about 1–1.5 TeV. As a consequence, the measurement of the cross section at large $M(VV)$ could provide information on the existence of the Higgs boson independently of its direct observation. In particular, absence of strong interactions in high energy boson-boson scattering could provide a strong incentive to probe harder for a light Higgs, which will require several years of data taking for a reliable discovery. But even if a Higgs particle is discovered, in this or other channels, it will be necessary to verify that indeed longitudinally polarized vector bosons are weakly coupled by studying boson-boson scattering in full detail.

The following vector boson fusion processes can be studied at LHC:

$$qq \to qqVV \to qqVZ \to qqqq\mu\mu/ee$$
$$qq \to qqVV \to qqVW \to qqqq\mu\nu/e\nu.$$

They offer a clear experimental signature, because of the presence of high p_T leptons from the W or Z decay, together with the highest branching ratio among the final states which are possible to reconstruct in an hadronic environment. In fact boson-boson scattering with a totally hadronic final state cannot be isolated from the non resonant QCD backgrounds whose cross section is much higher.

Final states where both bosons decay leptonically have been also analyzed:

$$qq \to qqVV \to qqZZ \to qq\mu\mu\mu\mu/qqeeee$$
$$qq \to qqVV \to qqZW \to qq\mu\mu\mu\nu$$
$$qq \to qqVV \to qqW^{\pm}W^{\pm} \to qq\mu^{\pm}\nu\mu^{\pm}\nu$$

They have a small rate but a very clear signature. Moreover in these channels both of the outgoing bosons can be unequivocally recognized as W or Z and this can be useful for the study of the cross section behavior at high boson-boson invariant mass. Finally in the $qqVV \to qqW^{\pm}W^{\pm} \to qq\mu^{\pm}\nu\mu^{\pm}\nu$ process the exact VV invariant mass cannot be reconstructed so an appropriate kinematic treatment is necessary. Nevertheless the study of this final state in the high

invariant mass region is very promising because in the $W^{\pm}W^{\pm} \rightarrow W^{\pm}W^{\pm}$ process the enhancement of the cross section due to the unitarity violation in the no-Higgs case is large.

All the listed channels have similar kinematic behavior. The particles in the final state coming from the decay of a W (or a Z) are expected to have quite high transverse momentum (p_T) and to be mostly produced centrally in the detector, i.e. at low absolute value of pseudo-rapidity (η). On the contrary, the two quarks that have radiated the vector bosons, the so called "spectator quarks", tend to go in the forward/backward regions at high $|\eta|$ and they have very large energy and p_T. Thanks to their peculiar kinematic pattern, the presence of these two spectator quarks is essential to tag the VV fusion events as a six fermions final state, therefore they also are called "tag quarks".

The most problematic background for the vector boson fusion signal in the semi-leptonic final state is the production of a single W (or Z) in association with n jets (n=2,3,4,5) which has a huge cross section (of the order of nanobarns). The background most difficult to reject in the totally leptonic channel is instead the production of a couple of bosons in association with n jets (n=0,1,2,3) with a cross section of some picobarns. Another potentially dangerous background with a big cross section is the QCD production of top pairs ($\simeq$ 200 pb). Lastly, the irreducible background coming from $\bar{t}t$ Electroweak production, Triple and Quartic Gauge Coupling (TCG,QGC) and non resonant 6 fermion final state, must be considered, which has a cross section of the same order as the signal and a very similar kinematic behavior.

For a complete overview of one of the analysis see e.g. [11]. In the following section some of the final state already accessible at low luminosity will be addressed as an example. In general, the discovery of the Higgs mass peak up to 500 GeV should require something more than 100 fb-1, while in the case of absence of the Higgs, due to the quite poor signal over background ratio, it is still difficult to say how long it will take to be able to relay only on the high $M(VV)$ region to understand the mechanism which breaks the symmetry, and high luminosity will surely be needed.

7.10.0.1 qqH with $H \rightarrow WW$

The analysis of the fully leptonic decay channel ($qql\nu l\nu$ final state) is similar to that described in the previous section (Sec. 7.9). This process has a lower cross section (50-250 fb) but the presence of the two additional quarks from the VBF, with high energy and pseudorapidity, can be exploited to disentangle the signal from the background.

The semileptonic decay channel ($qqqql\nu$ final state) has the advantage of a higher BR and it allows to reconstruct the Higgs mass peak. On the other hand

it suffers from very high background: double top ($\sigma \simeq 840\ pb$), single top ($\sigma \simeq 100\ pb$), double boson plus jets ($\sigma \simeq 100\ pb$) and single boson plus jets (σ bigger than 1 mb), to be compared with the $qqH \rightarrow qqWW$ cross section of about 0.6-2.7 pb. Thus strong cuts are necessary and this implies a good knowledge of the physics involved. However the cross sections of the multiple jets processes at the LHC scale are not yet very well known and they will be measured precisely only from the LHC data themselves. Moreover many systematics about the jets detection and reconstruction are still quite uncertain, they can be understood and measured only from the data.

The preliminary estimation of the significance with 30 fb^{-1} is shown in Figures 7.10 and 7.11(left).

7.10.0.2 qqH with $H \rightarrow \tau\tau$

This channel has been analyzed with one τ decaying into leptons and the other τ into hadrons ($\sigma \simeq$ 50-160 pb). The irreducible backgrounds are the QCD and EW production of two τ leptons from Z/γ^* with associated jets (QCD 2τ+2/3 jets $\sigma \simeq 1.6\ pb$, EW 2τ+2 jets $\sigma \simeq 230$ fb). The reducible backgrounds considered are the $W+$ multi-jet production (W+3/4 jets $\sigma \simeq 14.5$ pb with $W \rightarrow \mu\nu$) and $t\bar{t}$ events ($\sigma \simeq 86$ pb with $W \rightarrow l\nu$), in which one of the jets can be misidentified as a τ-jet.

This analysis has to reconstruct a very complex final state. The hadronically decaying τ is reconstructed from a little ($\Delta R = 0.4$) isolated jet. A very low impurity (2.7%) is obtained thanks to the selection cuts, costing a low reconstruction efficiency (30%). The energy resolution on the reconstructed τ is 11.3%. The leptonically decaying τ is recognized from the electron or muon with highest transverse momentum, requiring $p_T > 15\ GeV$. The τ energies are calculated using collinear approximation of visible part of τ decay products and neutrinos. A raw (not calibrated) missing transverse energy (MET) greater than 40 GeV is required. The MET resolution after all corrections is 20%, this is the largest contribution to the Higgs mass resolution. Finally the presence of the two quarks emitting the bosons in the VBF process can be exploited: they have very high energy and high rapidity gap (as shown in Figure 7.9) because there is not color exchange between them, being produced trough an EW process. After having removed the τ jet and the two VBF jets, a central jet veto is applied using a Monte Carlo jet energy calibration. The significance exceeds 3σ with 30 fb^{-1}, as reported in Figures 7.10 and 7.11(left). The number of events is measured directly from the data fitting the $M(\tau\tau)$ distribution. The uncertainty on the number of background events (7.8% with 30 fb^{-1}) is computed from its spread in 10.000 toy Monte Carlo data distributions generated following the fit results.

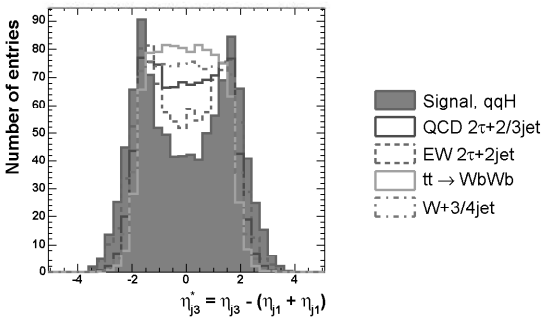

Figure 7.9: The pseudorapidity (η) distribution of the 3rd jet with respect to the two forward jets, $\eta^*_{j3} = \eta_{j3} - (\eta_{min} + \eta_{max})$, for the VBF $H \to \tau\tau$ signal and the various backgrounds in CMS. The total number of entries is normalized to 1000 events.

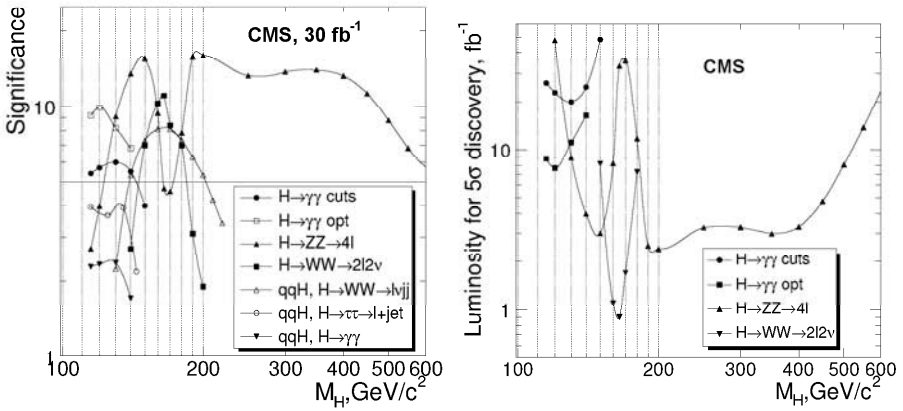

Figure 7.10: Significance achievable with 30 fb^{-1} (left) and luminosity needed for a 5σ discovery (right) in the various channels as a function of the Higgs mass with the CMS detector [13].

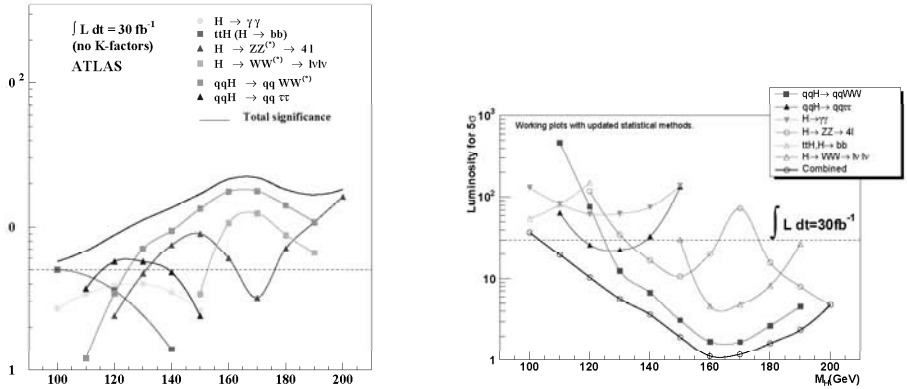

Figure 7.11: Significance achievable with 30 fb^{-1} (left) and luminosity needed for a 5σ discovery (right) in the various channels as a function of the Higgs mass with the ATLAS detector.

7.10.1 The Higgs signal Significance at LHC

Figure 7.10 and figure 7.11 (see ref. [13] and [14]) are a good summary of the CMS and ATLAS potential for the Higgs discovery with low luminosity.

The various channels will be combined to get a coherent picture. Depending on the Higgs mass and on the cross section $\times BR$ only 10 fb^{-1} or few years of data taking will be necessary to get a undiscussed significance. Figure 7.12 shows instead the ATLAS and CMS potential for the Higgs discovery including as well one year at high luminosity. In figure 7.13 the needed luminosity for a 95% exclusion and for a 5σ discovery are shown as a function of the Higgs boson mass. It should be noticed that a careful preliminary work must be done in order get those results: the first data will be used to study the detector systematics (in particular the control of the jets response and of the MET resolution will be difficult at the beginning) and to measure the cross sections of multi-jets background processes (mainly $t\bar{t}$ and single and double boson production in association with jets).

References

1. G. Ridolfi, "Search for the Higgs boson: theoretical perspective", hep-ph/0106300.

2. The LEP Collaborations, the LEP Electroweak Working Group and the

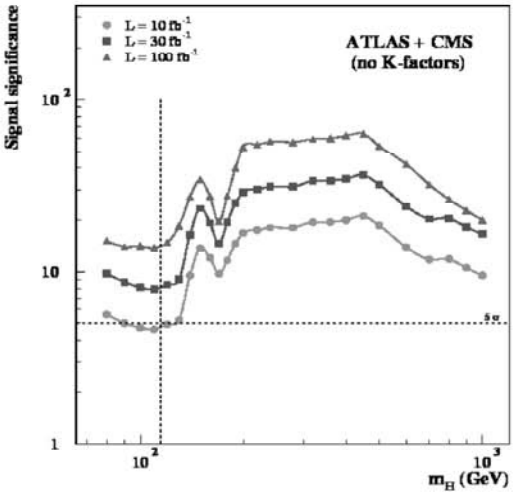

Figure 7.12: Significance achievable with 10, 30 and 100 fb^{-1} for the two experiment combined together.

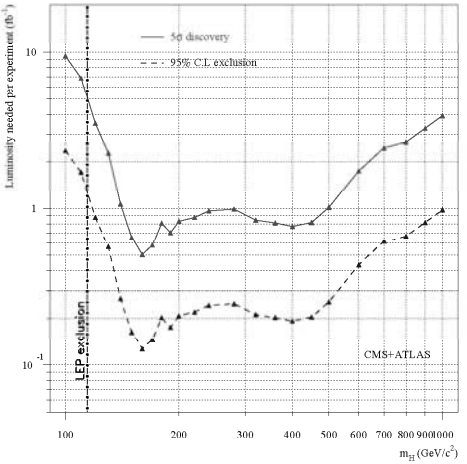

Figure 7.13: The needed luminosity for an exclusion at 95% CL or for a discoryat 5σ

SLD Heavy Flavour Group, "A combination of Preliminary Electroweak Measurements and Constraints on the Standard Model", LEPEWWG 2003-01.

3. The LEP Working Group for Higgs Boson Searches, "Search for the Standard Model Higgs boson at LEP", Phys. Lett. B 565(2003)61-75.

4. M. Spira, "HIGLU: a Program for the Calculation of the Total Higgs Production Cross Section at Hadron Collider via Gluon Fusion Including QCD Corrections", DESY T-95-05 (1995), hep-ph/9510347.

5. J. Pumplin, D. R. Stump, J. Huston, H. L. Lai, P. Nadolsky and W. K. Tung, "New generation of parton distribution with uncertainties from global QCD analysis", JHEP 0207:012, (The CTEQ Collaboration).

6. H. Georgi, S. Glashow, M. Machacek and D. Nanopulous, "Higgs Bosons from Two Gluon Annihilation in Proton Proton Collision", Phys Rev. Lett. 40, (1978) 692.

7. A. Djouadi, "The Anatomy of Electroweak Symmetry Breaking", LPT-Orsay 06-17 (2006), hep-ph/05031724.

8. R. Rainwater, M. Spira and D. Zeppenfeld, "Higgs Boson Production at Hadron Collider", hep-ph/0203187.

9. M. Kramer, E. Laenen and M. Spira, "Soft gluon radiation in Higgs boson production at the LHC", Nucl. Phys. B511 (1998) 523, hep-ph/9611272.

10. A. Djouadi, J. Kalinowski and M. Spira, "HDECAY; a Program for Higgs Boson Decay in the Standard Model and its Supersymmetric Extension", DESY 97-079 (1997), hep-ph/9704448.

11. N.Amapane et al., *Study of VV-scattering processes as a probe of electroweak symmetry breaking*, CMS AN 2007/005.

12. E. Gabrieli, F. .Maltoni, B. Mele, F. Piccinini and R. Pittau *Higgs Boson Production in Association with a Photon in Vector Boson Fusion at the LHC*, Nucl. Phys. B781 (2007) 64.

13. CMS Collaboration, Jour. Phys. G34 (2007) 1.

14. ATLAS Collaboration, hep-ph/0401148, ATLAS collaboration ATL-PHYS-2004-034.

15. ATLAS Physics TDR.